Deblending using normal moveout and median filtering in common-midpoint gathers[a]

[a]Published in Journal of Geophysics and Engineering, 11, 045012, (2014)

Yangkang Chen[*], *Jiang Yuan*[†], *Zhaoyu Jin*[‡], *Keling Chen*[§] *and Lele Zhang*[¶]

ABSTRACT

The benefits of simultaneous source acquisition are compromised by the challenges of dealing with intense blending noise. In this paper, we propose a processing workflow for blended data. The incoherent property of blending noise in the common-midpoint (CMP) gathers is utilized for applying median filtering along the spatial direction after normal moveout (NMO) correction. The key step in the proposed workflow is that we need to obtain a precise velocity estimation which is required by the subsequent NMO correction. Because of the intense blending noise, the velocity scan can not be obtained in one step. We can recursively polish both deblended result and velocity estimation by deblending using the updated velocity estimation and velocity scanning using the updated deblended result. We use synthetic and field data examples to demonstrate the performance of the proposed approach. The migrated image of deblended data is cleaner than that of blended data, and is similar to that of unblended data.

INTRODUCTION

The technique of simultaneous-source (sometimes called *multisource*) acquisition means firing more than one shot at nearly the same time regardless of their interference. In conventional acquisition, however, either the temporal shooting intervals or the spatial sampling intervals are large enough so that the interference between successive shots can be ignored. The multisource technique can reduce the acquisition period and at the same time can improve data quality because of the decreased spatial sampling interval (Berkhout, 2008). The benefits from simultaneous-source acquisition are compromised by the challenges in removing strong blending interference. Because of its economic benefits and technical challenges, this technique has attracted the attention of researchers in both industry and academia (Mahdad et al., 2011; Huo et al., 2012).

In blended acquisition, more than one source is shot simultaneously, regardless of their interactive interference. The term *source* denotes a shot array, which can contain all the shots in a conventional acquisition system. When more than one source is involved in acquisition, either a denser or a wider shot coverage can be obtained

for a given constant acquisition period. Figure 1a depicts two simultaneous sources shooting from the same position towards the same direction. In this case, a two-times denser coverage can be obtained. Figure 1b depicts two simultaneous sources far from each other shooting along the same direction, in which case, a two-times wider shot coverage can be obtained. The number of simultaneous sources can be even larger, yielding a much denser and wider shot coverage. The shooting sequence of the shots and the direction of each source can also be variable. It's natural, that the observed data will contain strong interference, and the more simultaneous sources involved, the more severe the interference will be. For the blended acquisition geometry as shown in Figure 1b we acquire blended data with strong interference, as shown in Figure 2b. Figure 2a shows the acquired data using conventional acquisition, supposing that the two sources in Figure 1b are fired with large-enough time interval.

There are two main ways to deal with the challenges posed by simultaneous-source acquisition. The first is to use a first-separate and second-process strategy (Chen et al., 2013), which is also known as "deblending" (Doulgeris et al., 2012). The other is to use direct imaging and waveform inversion by applying some constraints to attenuate the artifacts caused by interference (Verschuur and Berkhout, 2011; Dai et al., 2012). Although the direct imaging approach has achieved some encouraging results, the preferable way so far is still to focus on the separation of blended data into individual sources as if acquired conventionally.

Different filtering and inversion methods have been used previously to deblend seismic data. Filtering methods utilize the property that the coherency of the simultaneous-source data is not the same in different domains, thus we can get the unblended data by filtering out the randomly distributed blending noise in a particular domain, in which one source record is coherent and the other is not (Hampson et al., 2008; Mahdad et al., 2012; Huo et al., 2012). One choice is to transform seismic data from the common-shot domain to common-receiver, common-offset or common-midpoint domain. Inversion methods treat the separation problem as an estimation problem that aims at estimating the desired unblended data. Because of the ill-posed property of such estimation problems, a regularization term is usually required (Doulgeris and Bube, 2012). Moore et al. (2008), Akerberg et al. (2008) and Moore (2010) use a sparsity constraint in the Radon domain to regularize the inversion. A sparsity constraint is also used by Abma et al. (2010) to minimize the energy of incoherent events present in the blended data. Bagaini et al. (2012) compared two separation techniques for dithered slip-sweep (DSS) data using the sparse inversion method Moore (2010) and f-x predictive filtering (Canales, 1984; Chen and Ma, 2014), and found the advantage of inversion methods over random noise attenuation techniques. van Borselen et al. (2012) proposed to distribute all energy in the simultaneous shot records by reconstructing the individual shot records at their respective locations. Mahdad et al. (2012) introduced an iterative estimation and subtraction scheme that combines the properties of filtering and inversion methods and exploits the fact that characteristics of blending noise differs in different domains. In order to deal with the aliasing problem, Beasley et al. (2012) proposed the alternating projection method (APM), which chooses corrective projections to exploit data characteristics and claims to be

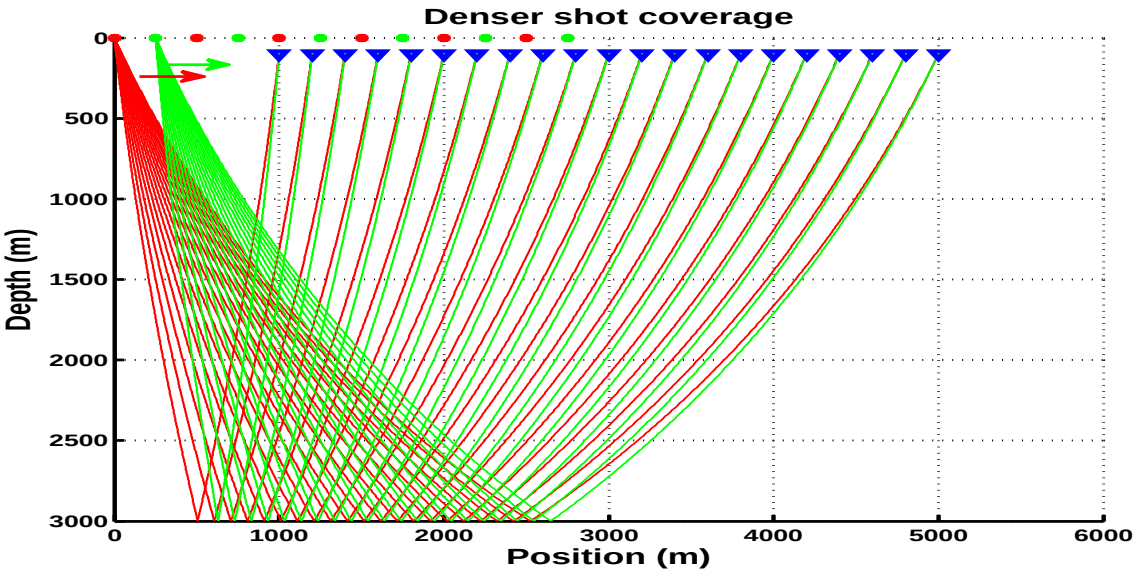

a

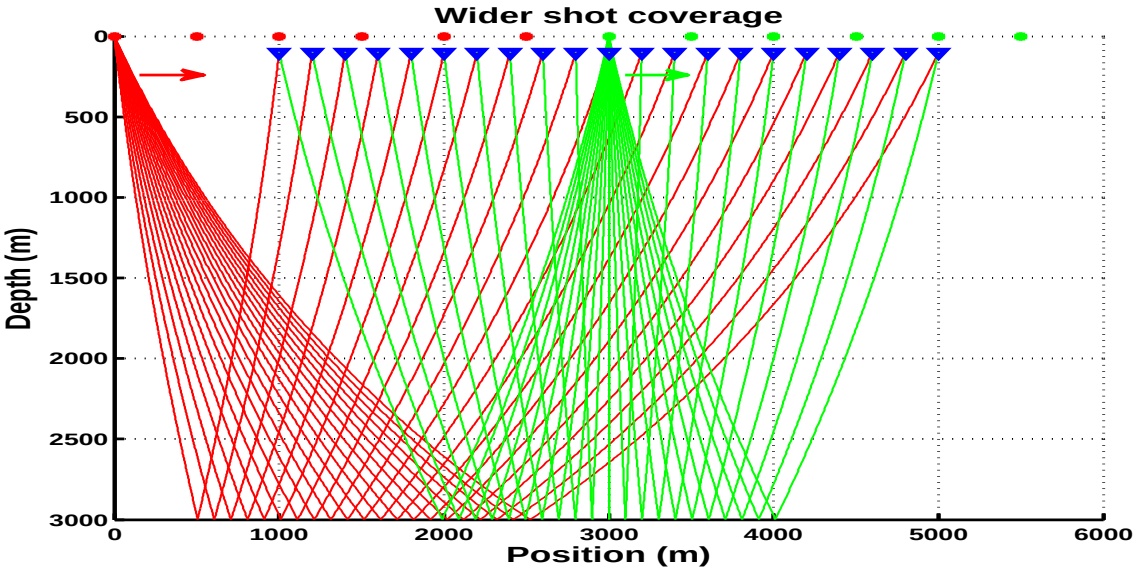

b

Figure 1: Demonstration for denser shot coverage (a) and wider shot coverage (b). Red points denote shot positions for source 1. Green points denote shot positions for source 2. Blue points denote receiver positions. Red and green strings denote the shooting rays. Arrows denote the shooting directions.

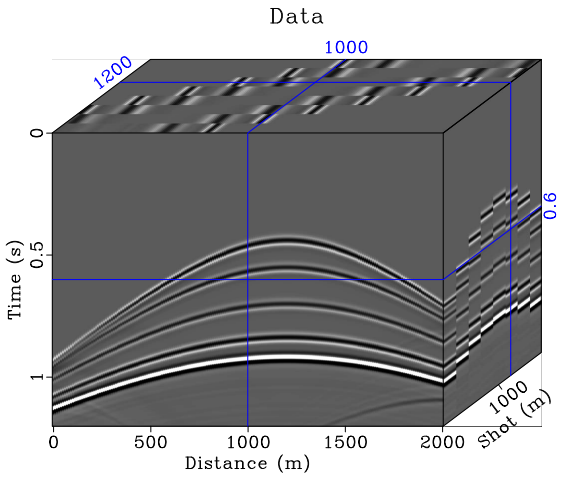

a

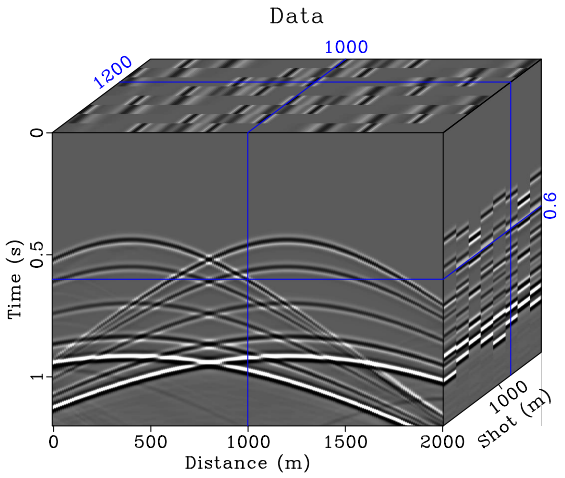

b

Figure 2: (a) Unblended data. (b) Blended data.

less sensitive to aliasing than other approaches.

Median filtering is notable for its ability to remove spiky noise and is also suitable to remove blending noise. However, median filtering can be applied only to seismic profiles containing horizontal events, otherwise it will harm much of the useful energy. In this paper, we propose to implement median filtering to attenuate blending noise after normal moveout in common-midpoint (CMP) gathers. The deblending can be inserted into a conventional processing workflow . The benefits of the proposed deblending approach are its easy implementation and efficient improvement for the migrated image without use of iterative deblending, which is extremely time-consuming. Synthetic and field data examples demonstrate the effectiveness of the deblending method and improvement for the final migrated image.

METHOD

Independent marine-streamer simultaneous shooting (IMSSS)

As shown in Figure 3, our blended survey is based on independent marine-streamer simultaneous shooting (IMSSS). Figure 3 shows four independent marine-streamer sources. Note that the number of simultaneous sources need not be limited to four. They shoot independently as in the conventional way and yield their own data. For a 3D seismic survey, the IMSSS can help cover a 2D surface area efficiently. With four sources, the efficiency is increased by four times. The increased efficiency, however, is compromised by interference among the four sources.

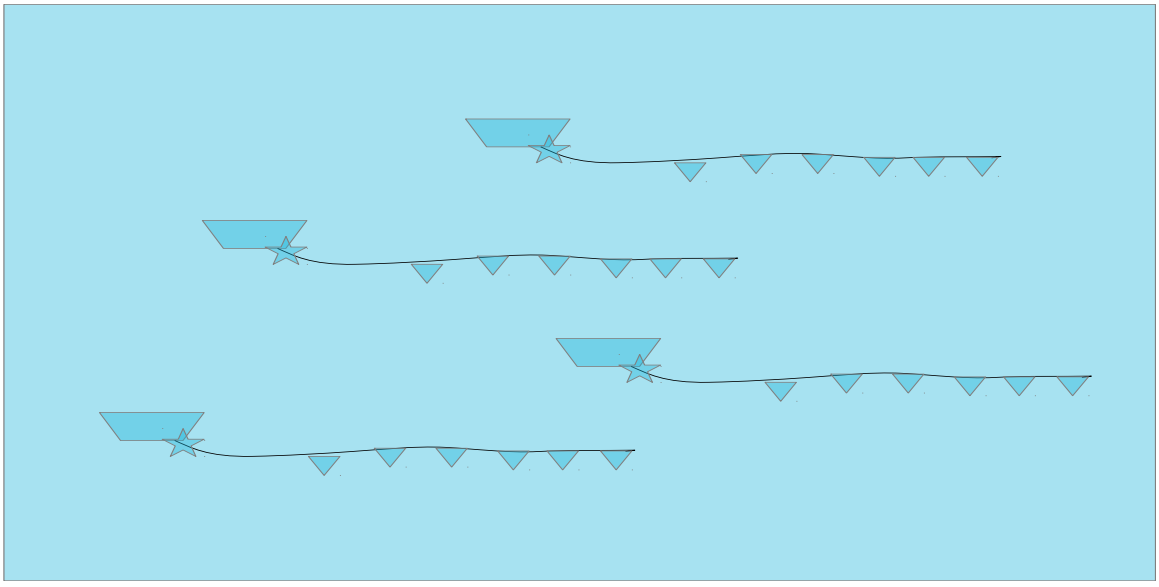

Figure 3: Demonstration of independent marine-streamer simultaneous shooting (IMSSS).

Transformation between different domains

The coherency of simultaneous-source data is not the same in different domains. The interference appears coherent in common-shot gathers (CSG); however, the interference turns out to be incoherent when observed in common-midpoint gathers (CMG), common-offset gathers (COG) and common-receiver gathers (CRG).The transformation from shot-receiver domain to midpoint-half-offset domain can be realized by the following equations:

$$\mathbf{m} = \frac{\mathbf{s} + \mathbf{r}}{2}, \tag{1}$$

$$\mathbf{h} = \frac{\mathbf{r} - \mathbf{s}}{2}, \tag{2}$$

where $\mathbf{m}$, $\mathbf{s}$ and $\mathbf{r}$ denote the coordinates of midpoint, shot, and receiver, respectively. $\mathbf{h}$ denotes the half-offset (with sign).

The transformation from shot-offset domain (the acquired data from marine streamer) to midpoint-half-offset domain can be realized by the following equations:

$$\mathbf{m} = \mathbf{s} + \frac{\mathbf{h}'}{2}, \tag{3}$$

$$\mathbf{h} = \frac{\mathbf{h}'}{2}, \tag{4}$$

where $\mathbf{h}'$ denotes the full offset.

Figure 4a shows synthetic shot-offset domain unblended data simulated from marine-streamer acquisition. Figure 4b shows the corresponding shot-offset-domain blended data using the IMSSS blended acquisition (with two sources). We can observe that the interference from the other source appears to be coherent in CSG. After transformation from the shot-offset domain to the midpoint-half-offset domain, the blending noise becomes random and spike-like, as shown in Figure 4c. Then deblending problem thus turns into a common denoising problem. Thus, in this section of examples, we focus on removing spiky noise in CMG. In the following sections, CSG also refers to the shot-offset domain and CMG also refers to the midpoint-half-offset domain.

Median filtering

Conventional median filtering is based on a scalar-value sorting process. When a set of scalars is sorted into an ascending or descending sequence, the middle value is chosen as standard for this sequence. In signal-processing or geophysical data analysis fields, this filter is commonly used to remove spiky noise. The more general mathematical

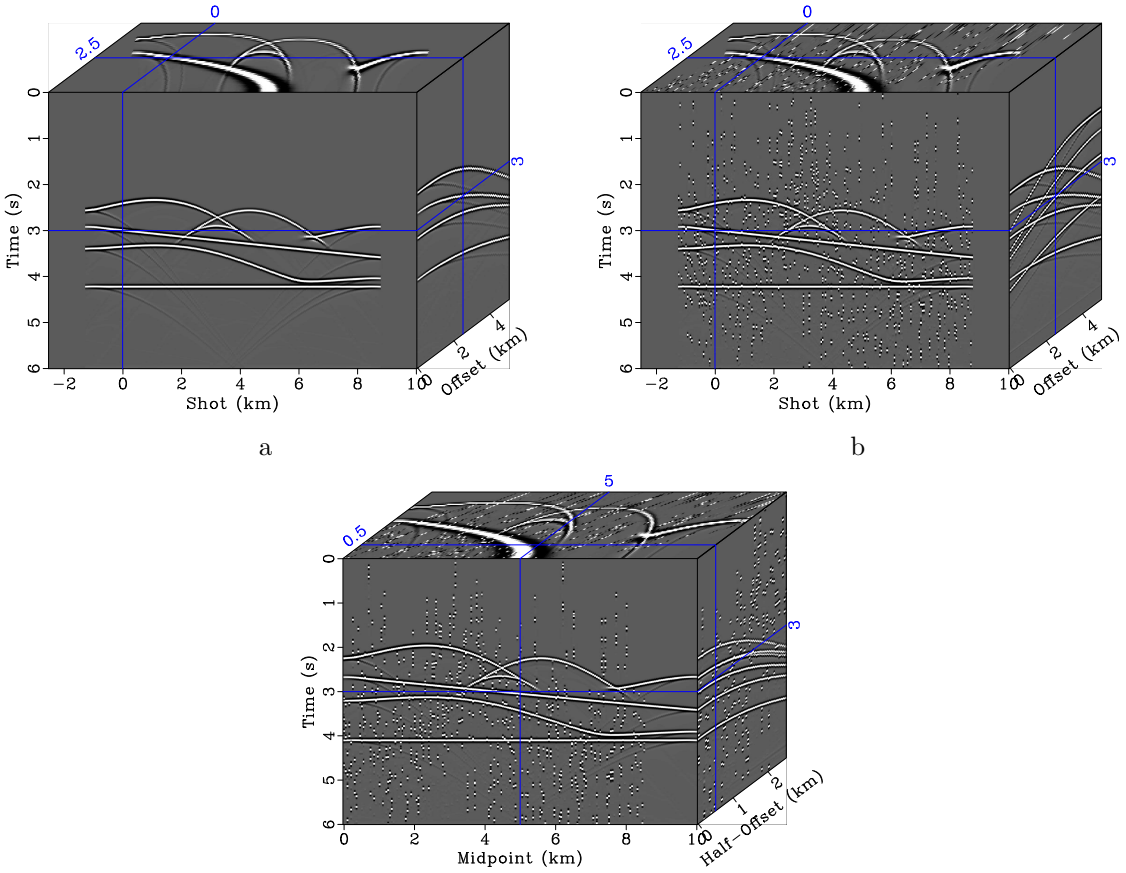

Figure 4: (a) Unblended data in the shot-offset domain. (b) Blended data in the shot-offset domain. (c) Blended data in the midpoint-half-offset domain.

formulation of median filtering is given as:

$$\hat{u}_{i,j} = \arg \min_{u_m \in U_{i,j}} \sum_{l=1}^{L} \|u_m - u_l\|_p, \tag{5}$$

where $\hat{u}_{i,j}$ is the output value for location $x_{i,j}$, $U_{i,j} = \{u_1, u_2, \cdots, u_L\}$, i, j are the position indices in a 2-D profile, and l and m are both indices in the filtering window. L is the length of the filtering window, and p denotes L_p norm. Commonly $p = 1$ corresponds to standard median filtering.

Unlike 2D signalprocessing , where the signal is multi-dimensionally coherent, geophysical data are only spatially coherent. Because of the temporally sparse property, the useful signal turns into a spike-like form. This spatial coherent characteristic requires that conventional median filtering should be taken along the spatial direction. Here, spatial direction means the horizontal direction for a 2D seismic profile. In addition, the local slope of an event should be small in order to preserve more useful energy. Figure 5 shows the effectiveness of median filtering in attenuating blending noise and preserving useful events. Figure 5b corresponds to median filtering along the time direction with a filter length of 11. With this choice, most of the useful energy has been removed. Figure 5c corresponds to median filtering along the spatial direction with a filter length of 7. Figure 5d corresponds to median filtering along the spatial direction with a filter length of 11. When the filter length is set at 7, most of horizontal energy is preserved and some dipping energy is lost. When the filter length is set at 11, most of the dipping energy is lost. Thus, we conclude that using median filtering in a profile with dipping events is dangerous; if the filter length is not appropriately chosen, the energy loss is heavy.

For dipping events, multidimensional median filtering can be used as a substitute (Huo et al., 2012). Multidimensional median filtering, however, requires a precise estimation of the local slope of the seismic events, which may be difficult in field-data processing in the presence of intense random or spiky noise. Besides, using multidimensional median filtering needs much more computational cost and memory. Here, we propose using median filtering after NMO in the CMG, where the events are flatten and the effectiveness of median filtering is maximized.

Median filtering after NMO

By utilizing the effectiveness of median filtering in removing spike-like noise and inserting median filtering into a common seismic processing workflow, we propose the following new processing workflow:

1. Transform the blended data from CSG to CMG.
2. Apply velocity scan and pick the NMO velocity.
3. Apply normal moveout.

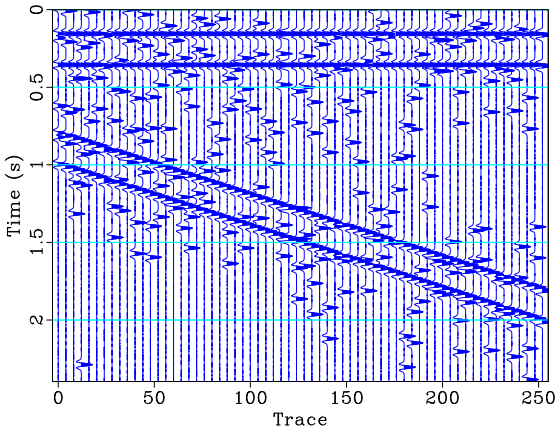
Time (s)
0
0.5
1
1.5
2
0
50
100
150
200
250
Trace

a

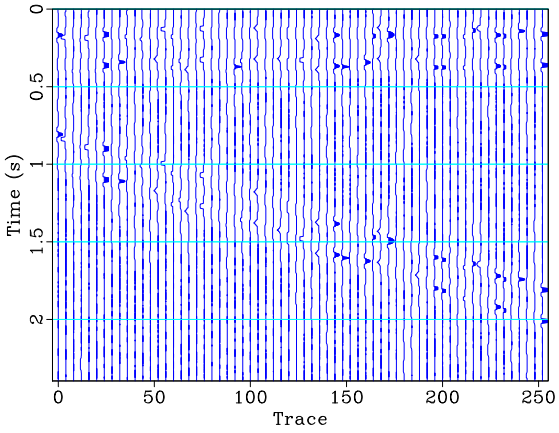
Time (s)
0
0.5
1
1.5
2
0
50
100
150
200
250
Trace

b

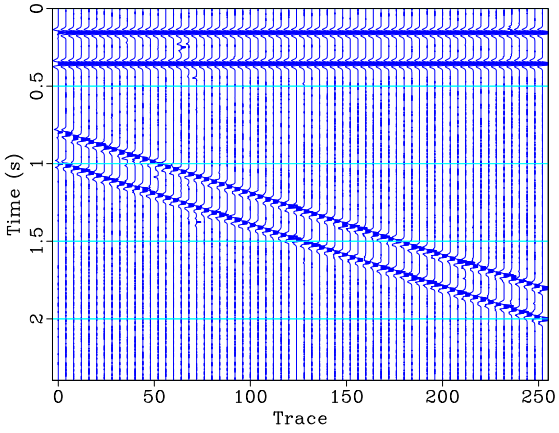
Time (s)
0
0.5
1
1.5
2
0
50
100
150
200
250
Trace

c

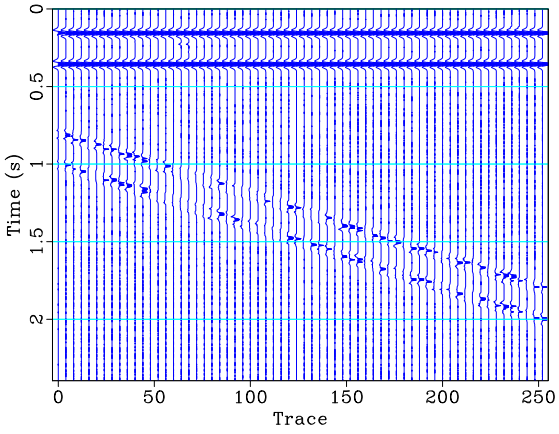
Time (s)
0
0.5
1
1.5
2
0
50
100
150
200
250
Trace

4. Apply median filtering along the offset direction in CMG.
5. Apply inverse normal moveout.
6. Prestack migration in CMG or transform back to CSG for other processing tasks.

The key point in the above workflow is flattening the seismic events in order to apply median filtering, which results from obtaining a convincing velocity scan. Because of the intense blending noise, the velocity scan could not be obtained in one step. To solve the problem, we may need to implement steps 2-4 recursively in order to get a better velocity scan. Two velocity scanning iterations are usually adequate to get an acceptable velocity. The proposed processing flow can recursively polish both deblended result and velocity estimation. On one hand, the better velocity estimation can help to make the NMO-corrected events flatter, which improve the performance of median filtering to remove blending noise and to preserve useful energy. On the other hand, the better deblended result can also help to improve the velocity estimation.

EXAMPLES

The first example is a single synthetic CMP gather. The clean unblended data, blended data, and velocity scan of the blended data are shown in Figures 6a, 6b, and 6c, respectively. Figure 7 shows the blended data after NMO correction and deblended data after NMO correction and median filtering. The median filtering is effective in that most of the interferences have been removed. After inverse NMO on Figure 7b, the deblended data in CMP gather is shown in Figure 8a. The blending noise section is shown in Figure 8b. From the deblending error section as shown in Figure 8c, we conclude that the proposed method can achieve an excellent result, because the deblending error is small.

We now provide two examples to demonstrate the performance of the proposed workflow described previously. In the next two examples, we use two sources to simulate the blended data. The second example is based on a simple synthetic dataset, which contains four reflectors. The velocity in the model is linearly increasing along the depth axis. We use Kirchhoff modeling to simulate the CSG and blend the data according to IMSSS. After common velocity-semblance scanning, we can pick the NMO velocity and apply NMO. Applying median filtering with a 9-point filter length along the offset direction removes the blending noise. By inverse NMO, we get the deblended dataset in the common-midpoint domain. Figure 9 shows the comparison of CMGs. Figure 10 shows the comparison of velocity scan, in which we see the velocity scan for the blended CMG is smeared along with the noise. After scanning the deblended data coming from the first rough velocity scan and first NMO correction, we however obtain a convincing velocity map. Using the updated NMO with new velocities, we get flatter events that are more suitable for median filtering. Figure 11 shows the comparison of migrated images. In this example, we use prestack

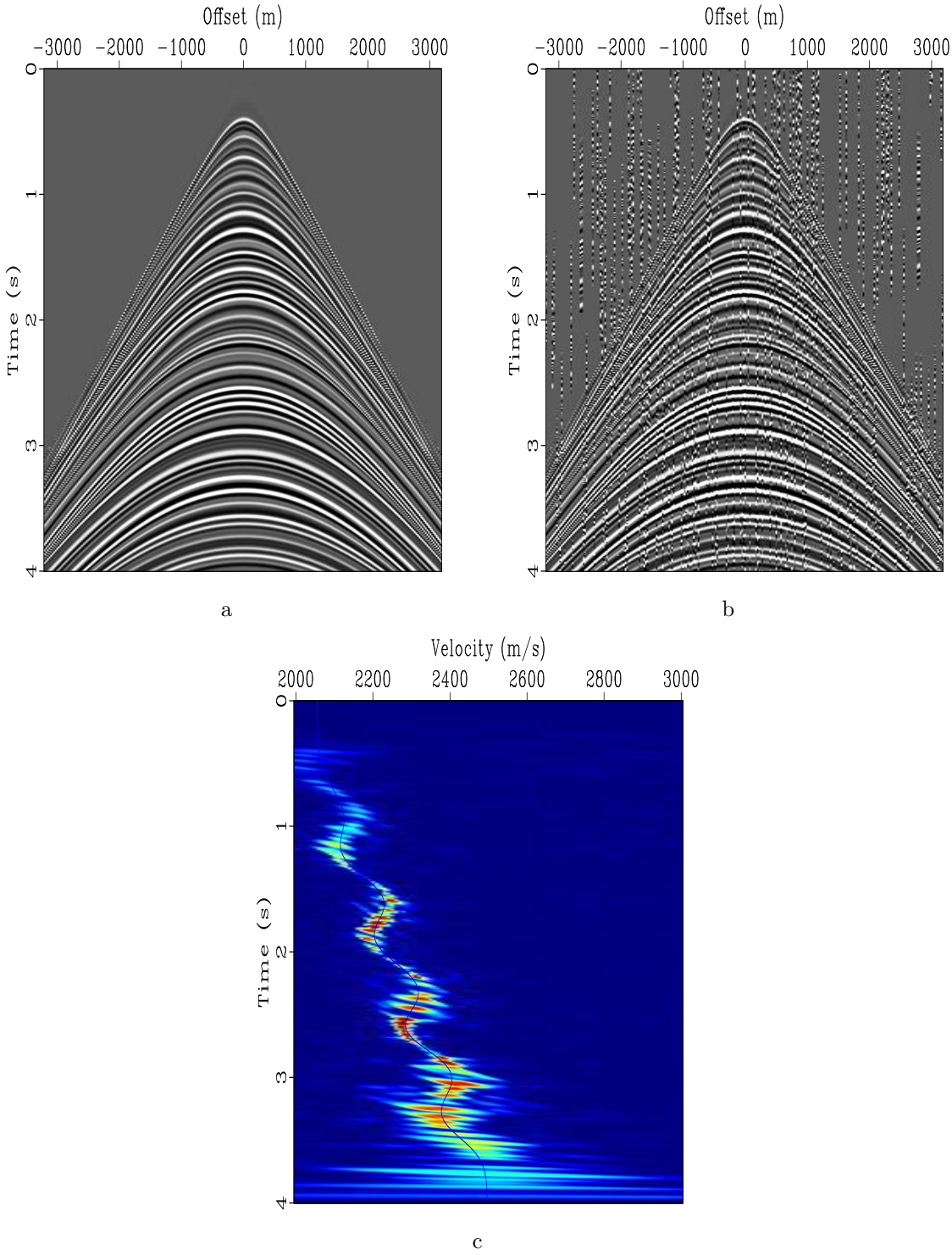

Figure 6: (a) Clean CMP gather. (b) Blended CMP gather. (c) Velocity scan for blended CMP gather.

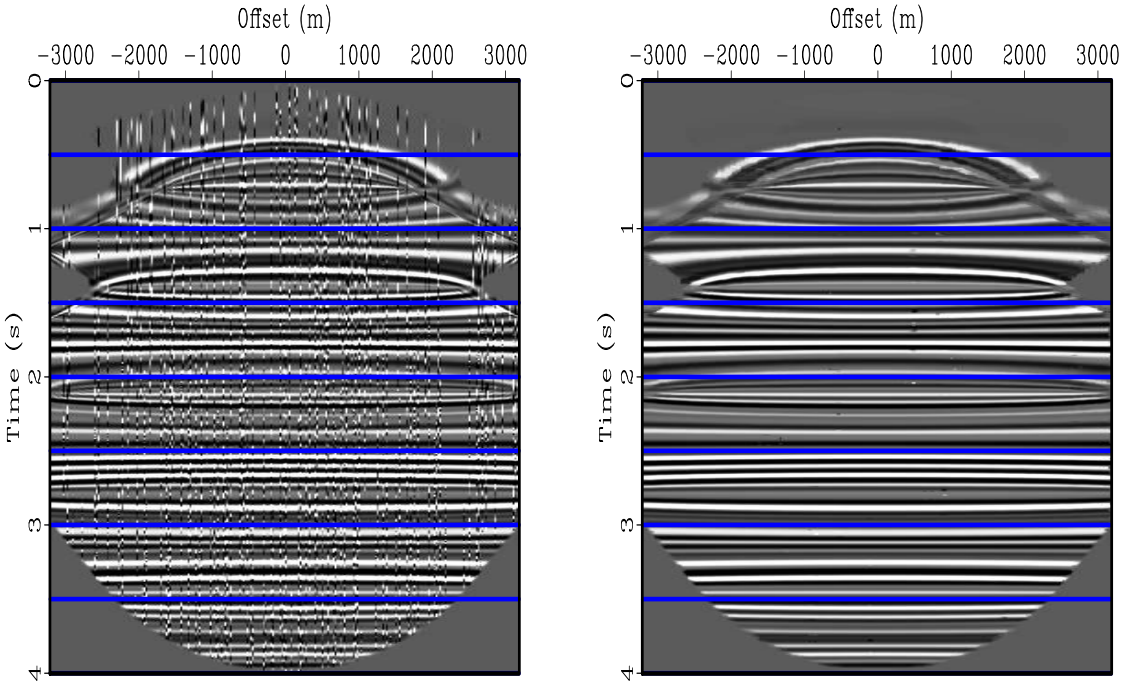

a b

Figure 7: (a) CMP gather after NMO. (b) CMP gather after NMO and median filtering.

kirchhoff time migration (PSKTM) (Docherty, 1991) as the migration operator. We then use Dix inversion (Dix, 1955) to convert the time image to depth image. The migrated image after deblending is much cleaner than that of the blended data.

The third example is a marine field dataset from the Gulf of Mexico. Figure 12 shows the comparison of CMGs. Figure 13 shows the comparison of velocity scans. Figure 14 shows the comparison of the migrated image. In this example, we use the same migration approach to obtain the seismic images. We have the similar observation to that for the second example: the migrated image for the deblended data is cleaner, especially for the shallow part, indicated by the arrows and frame boxes. For a better view, we zoom the parts indicated by frame boxes and show them in Figure 15. It's obvious to see the improvement for the final migrated image after using the proposed deblending approach.

CONCLUSIONS

We have proposed a basic workflow for dealing with blended data. The processing domain is in CMG, where blending noise appears to be incoherent and seismic reflections appear as hyperbolic events. By applying median filtering along the spatial direction after NMO in CMG, we can easily remove the blending noise without harm-

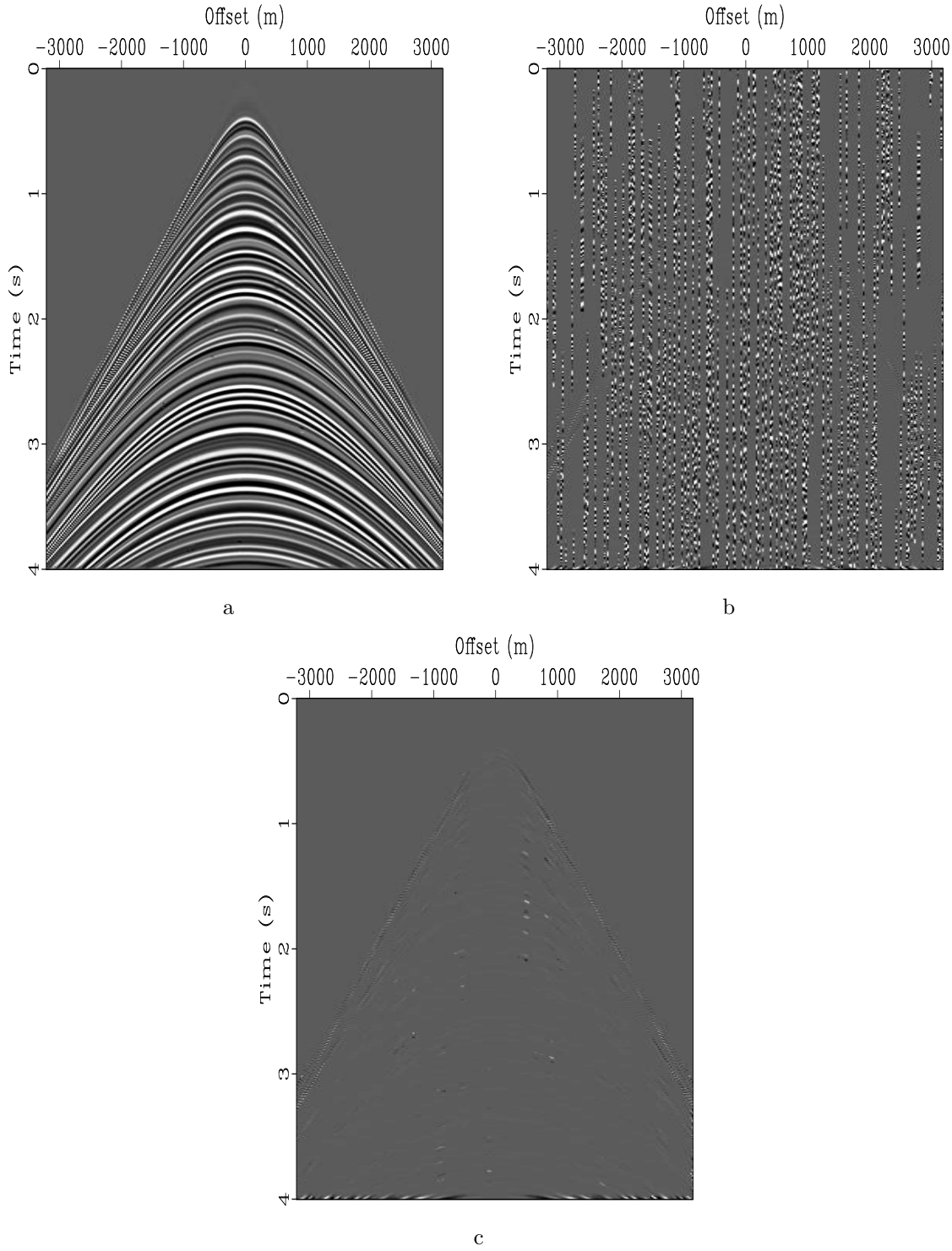

Figure 8: (a) CMP gathering after deblending. (b) Blending noise section. (c) Deblending error section.

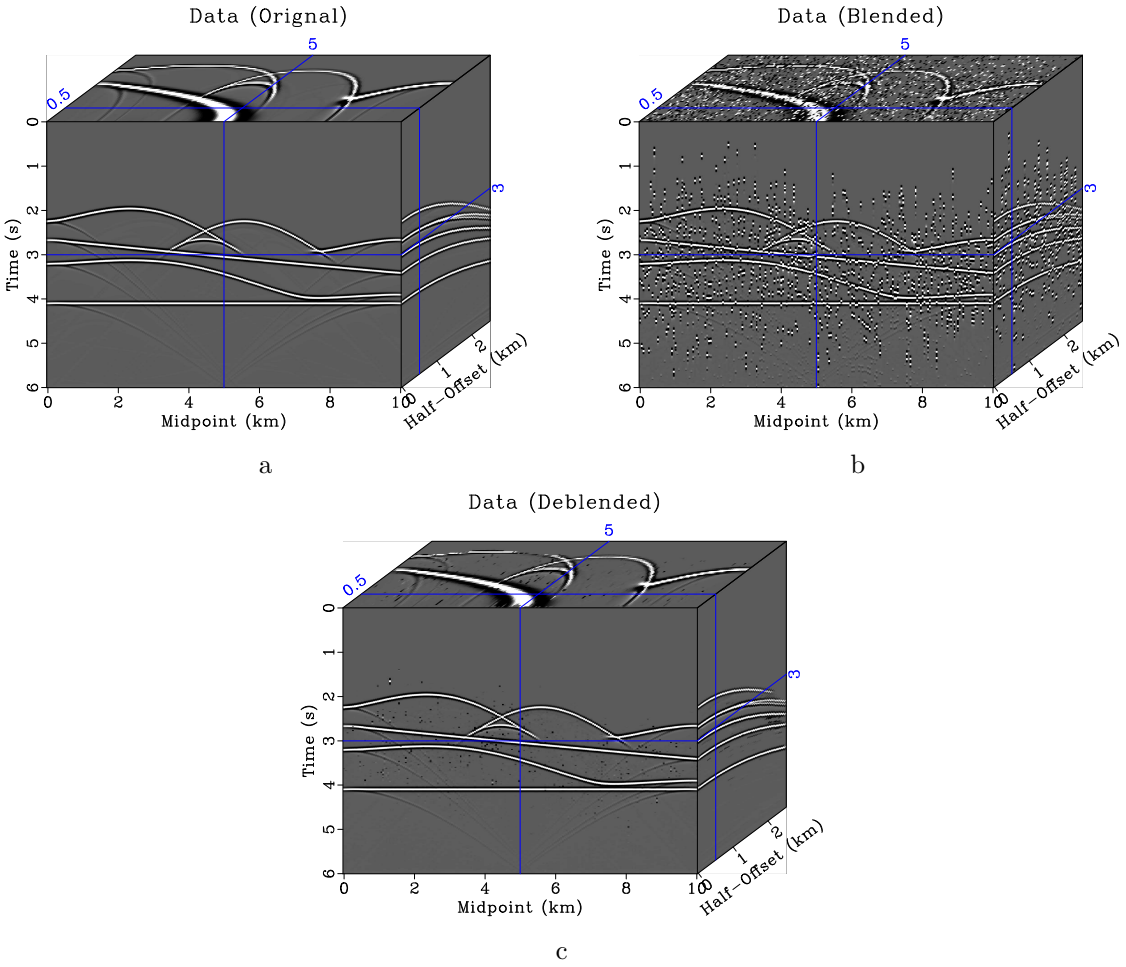

Figure 9: Comparison of CMP gathers. (a) Original unblended CMP gathers. (b) Blended CMP gathers. (c) Deblended CMP gathers.

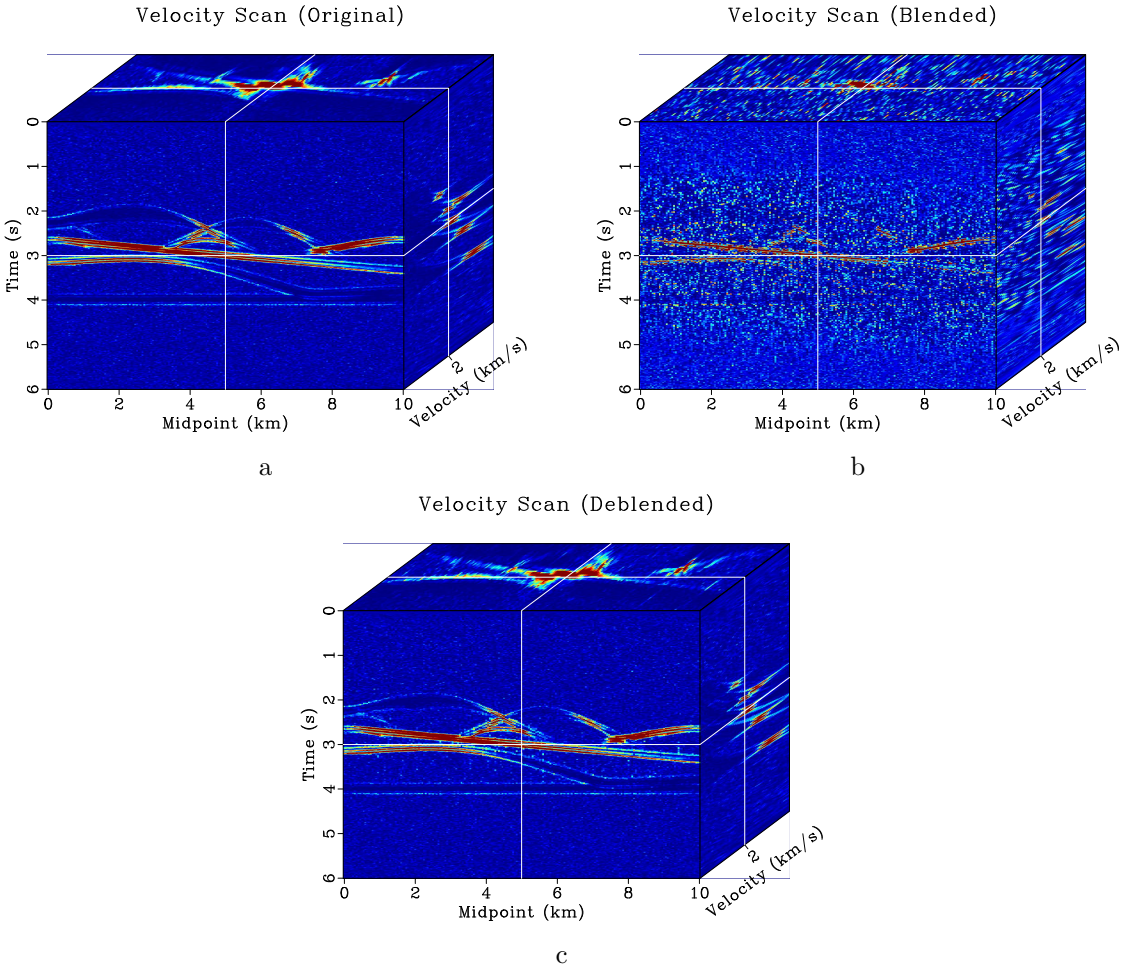

Figure 10: Comparison of velocity scans. (a) Velocity scan for original unblended data. (b) Velocity scan for blended data. (c) Velocity scan for deblended data.

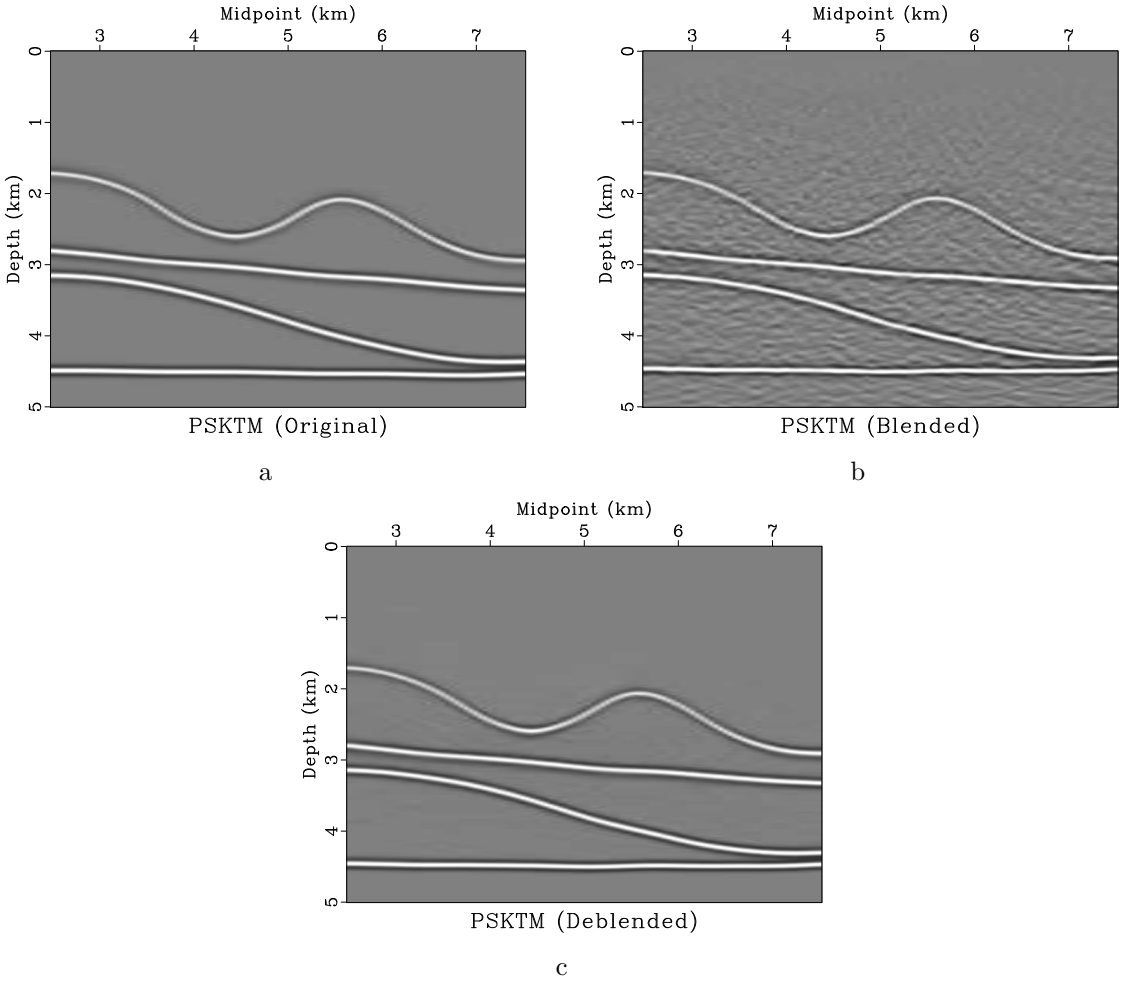

Figure 11: Comparison of migrated images using prestack Kirchhoff time migration (PSKTM). (a) Migrated image for unblended data. (b) Migrated image for blended data. (c) Migrated image for deblended data.

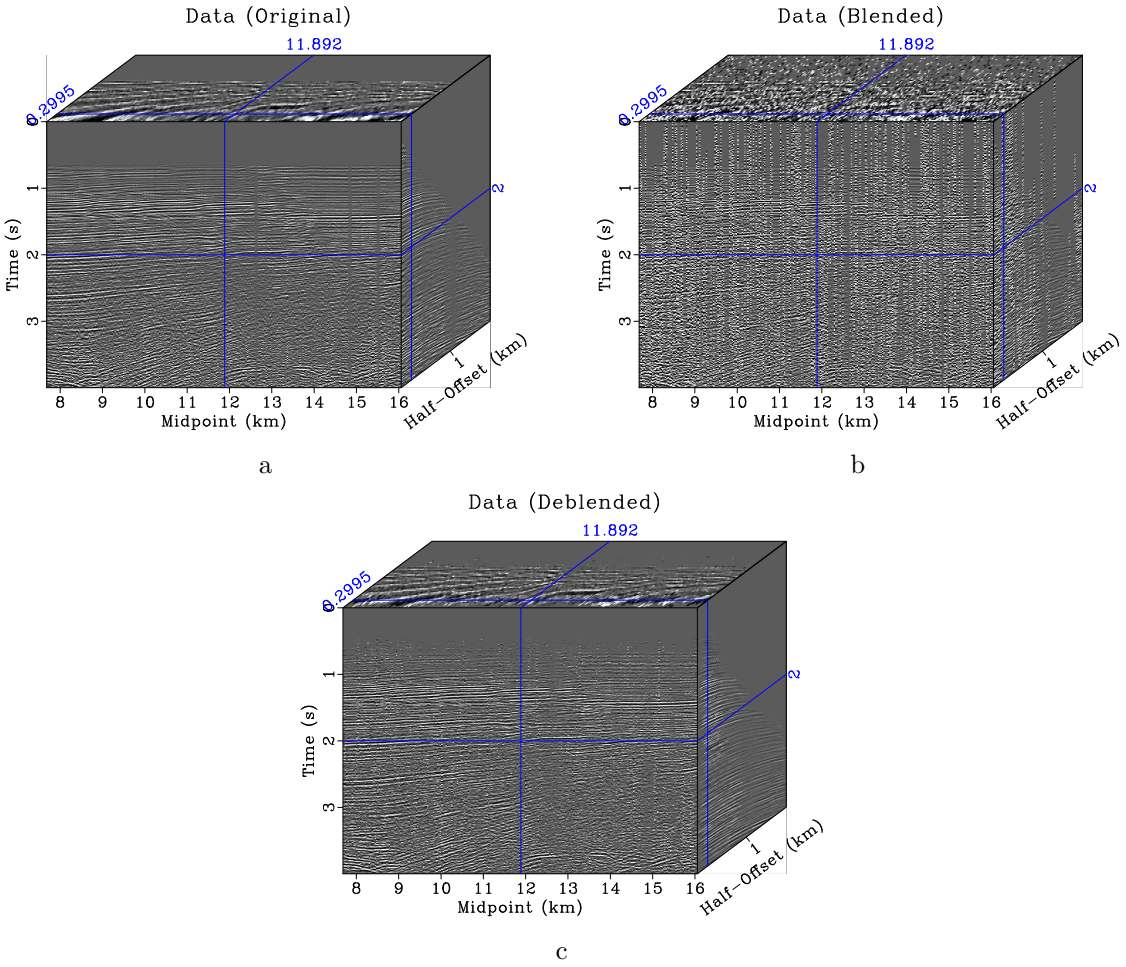

Figure 12: Comparison of CMP gathers. (a) Original unblended CMP gathers. (b) Blended CMP gathers. (c) Deblended CMP gathers.

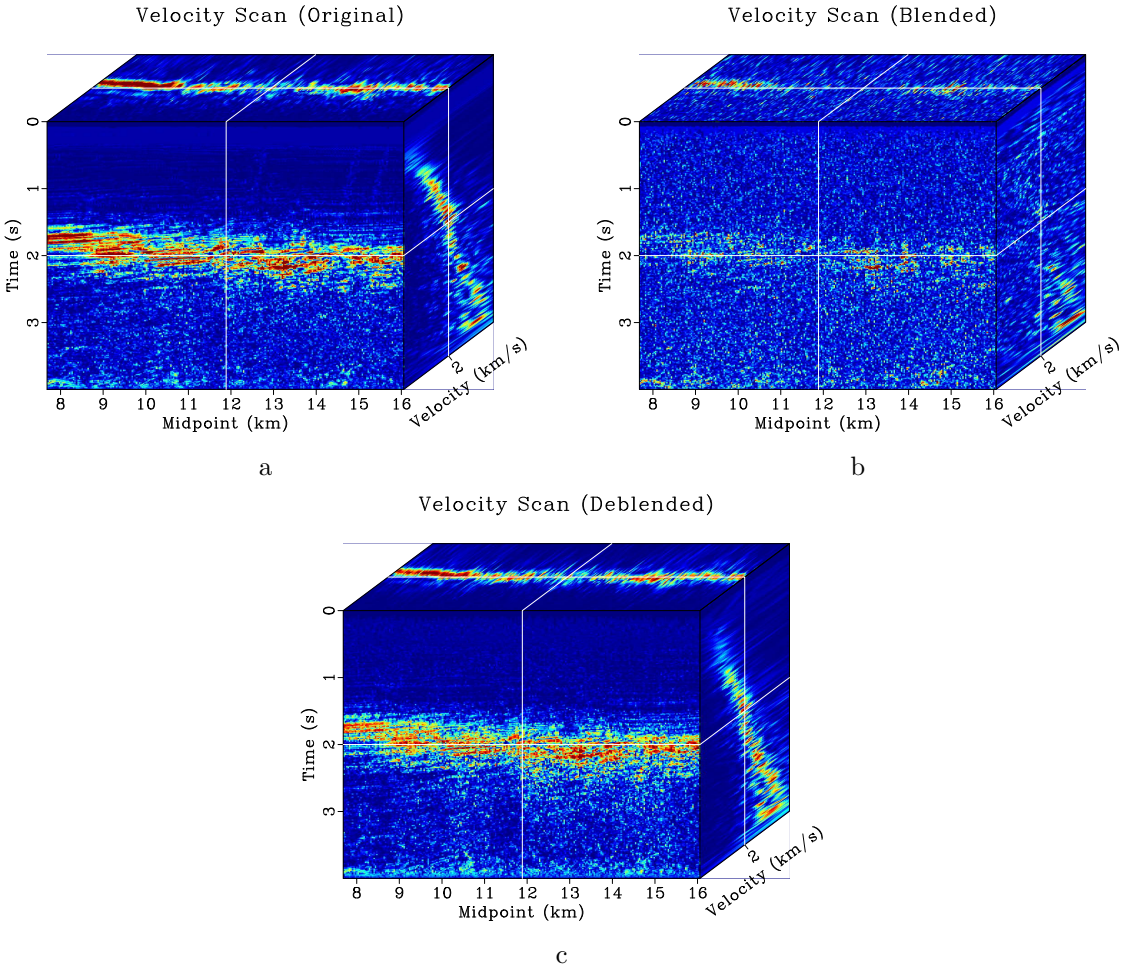

Figure 13: Comparison of velocity scans. (a) Velocity scan for original unblended data. (b) Velocity scan for blended data. (c) Velocity scan for deblended data.

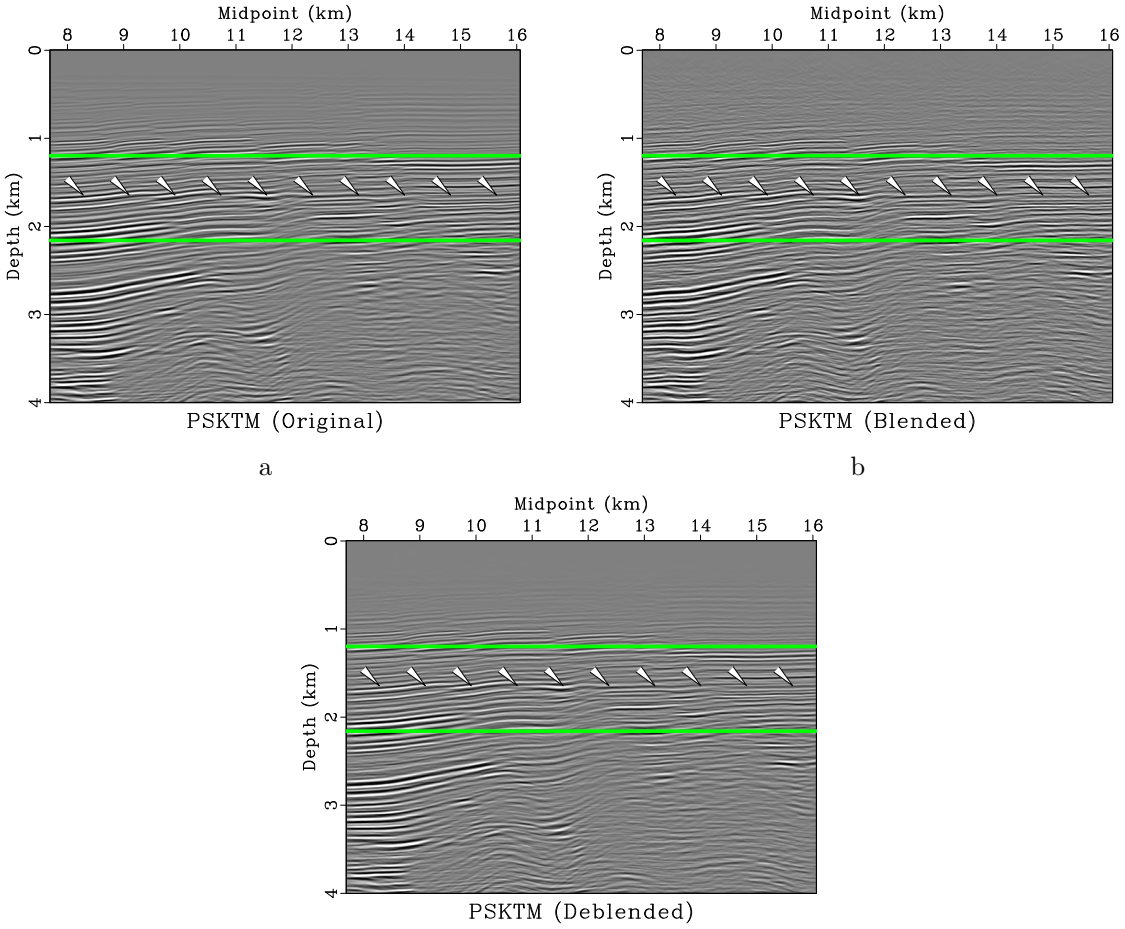

Figure 14: Comparison of migrated images using prestack Kirchhoff time migration (PSKTM). (a) Migrated image for unblended data. (b) Migrated image for blended data. (c) Migrated image for deblended data.

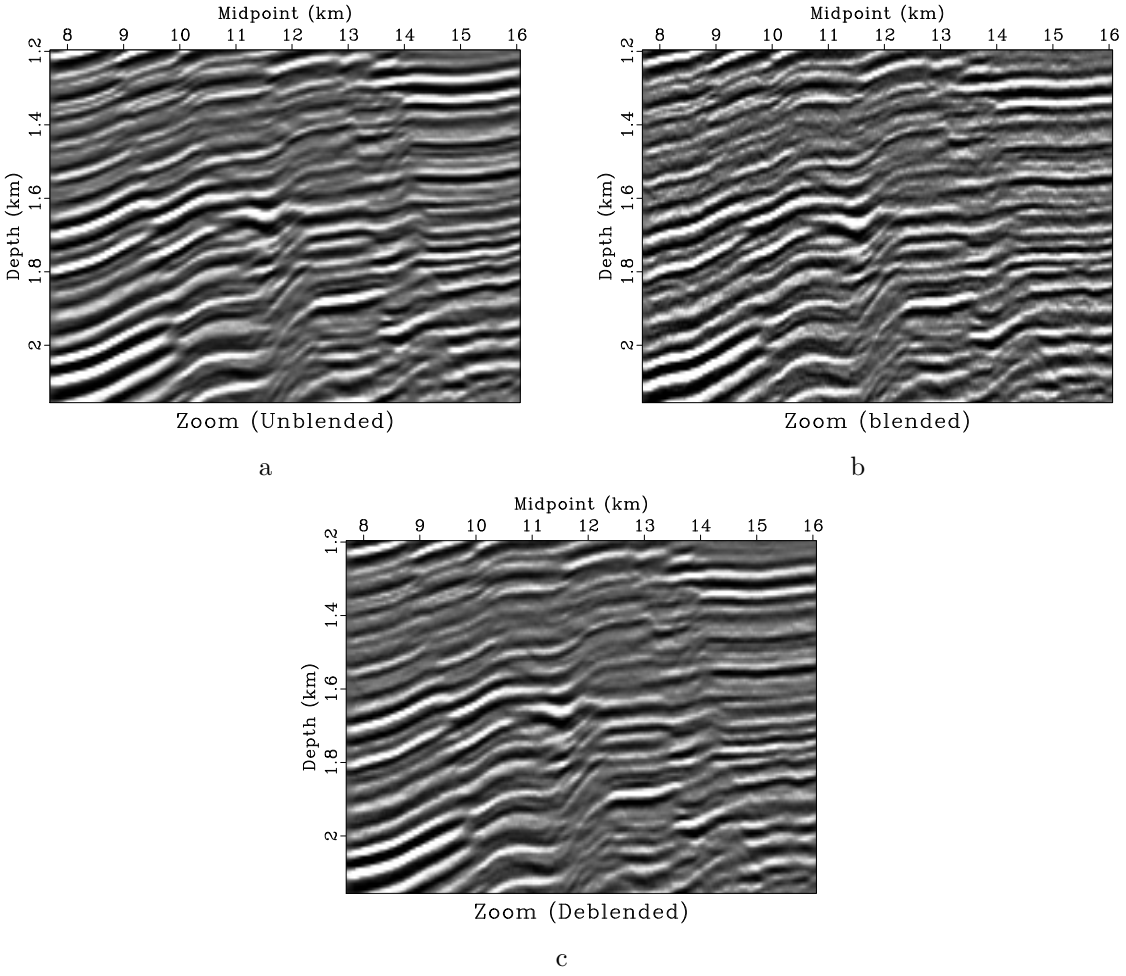

Figure 15: Comparison of zoomed migrated images using prestack Kirchhoff time migration (PSKTM). (a) Zoomed migrated image for unblended data. (b) Zoomed migrated image for blended data. (c) Zoomed migrated image for deblended data.

ing useful signal. By applying inverse NMO, we can get the deblended data. In order to obtain convincing velocity estimation, we use a recursive strategy. We polish both deblended result and velocity estimation by deblending using the updated velocity estimation and velocity scanning using the updated deblended result. It is readily implemented because we use a conventional version of median filtering and don't use any other sophisticated technique to aid in the deblending process. The migrated image of the deblended data shows cleaner structure than that of blended data, which confirms the effectiveness of the proposed deblending approach.

ACKNOWLEDGMENTS

Yangkang Chen would like to thank FairfieldNodal for the opportunity for a summer internship. We also thank Sergey Fomel, Josef Paffenholz and Araz Mahdad for inspiring discussions and helpful suggestions. We thank developers of Madagascar open-source platform for providing accessible codes.

REFERENCES

Abma, R. L., T. Manning, M. Tanis, J. Yu, and M. Foster, 2010, High quality separation of simultaneous sources by sparse inversion: 72nd Annual International Conference and Exhibition, EAGE, Extended Abstracts.

Akerberg, P., G. Hampson, J. Rickett, H. Martin, and J. Cole, 2008, Simultaneous source separation by sparse radon transform: 78th Annual International Meeting, SEG, Expanded Abstracts, 2801–2805.

Bagaini, C., M. Daly, and I. Moore, 2012, The acquisition and processing of dithered slip-sweep vibroseis data: Geophysical Prospecting, **60**, 618–639.

Beasley, C. J., B. Dragoset, and A. Salama, 2012, A 3d simultaneous source field test processed using alternating projections: a new active separation method: Geophysical Prospecting, **60**, 591–601.

Berkhout, A. J., 2008, Changing the mindset in seismic data acquisition: The Leading Edge, **27**, 924–938.

Canales, L., 1984, Random noise reduction: 54th Annual International Meeting, SEG, Expanded Abstracts, 525–527.

Chen, Y., S. Fomel, and J. Hu, 2013, Iterative deblending of simultaneous-source seismic data using shaping regularization: 83rd Annual International Meeting, SEG, Expanded Abstracts, 119–125.

Chen, Y., and J. Ma, 2014, Random noise attenuation by *f-x* empirical mode decomposition predictive filtering: Geophysics, **79**, V81–V91.

Dai, W., P. Fowler, and G. T. Schuster, 2012, Multi-source least-squares reverse time migration: Geophysical Prospecting, **60**, 681–695.

Dix, C. H., 1955, Seismic velocities from surface measurements: Geophysics, **20**, 68–86.

Docherty, P., 1991, A brief comparison of some kirchhoff integral formulas for migration and inversion: Geophysics, **56**, 1164–1169.

Doulgeris, P., and K. Bube, 2012, Analysis of a coherency-constrained inversion for the separateion of blended data: discovering the leakage subspace: 74th Annual International Conference and Exhibition, EAGE, Extended Abstracts.

Doulgeris, P., K. Bube, G. Hampson, and G. Blacquiere, 2012, Covergence analysis of a coherency-constrained inversion for the separation of blended data: Geophysical Prospecting, **60**, 769–781.

Hampson, G., J. Stefani, and F. Herkenhoff, 2008, Acquisition using simultaneous sources: The Leading Edge, **27**, 918–923.

Huo, S., Y. Luo, and P. G. Kelamis, 2012, Simultaneous sources separation via multidirectional vector-median filtering: Geophysics, **77**, V123–V131.

Mahdad, A., P. Doulgeris, and G. Blacquiere, 2011, Separation of blended data by iterative estimation and subtraction of blending interference noise: Geophysics, **76**, Q9–Q17.

———, 2012, Iterative method for the separation of blended seismic data: discussion on the algorithmic aspects: Geophysical Prospecting, **60**, 782–801.

Moore, I., 2010, Simultaneous source - processing and applications: 72th Annual International Conference and Exhibition, EAGE, Extended Abstracts.

Moore, I., B. Dragoset, T. Ommundsen, D. Wilson, C. Ward, and D. Eke, 2008, Simultaneous source separation using dithered sources: 78th Annual International Meeting, SEG, Expanded Abstracts, 2806–2809.

van Borselen, R., R. Baardman, T. Martin, B. Goswami, and E. Fromyr, 2012, An inversion approach to separating sources in marine simultaneous shooting acquision-application to a gulf of mexico data set: Geophysical Prospecting, **60**, 640–647.

Verschuur, D. J., and A. J. Berkhout, 2011, Seismic migration of blended shot records with surface-related multiple scattering: Geophysics, **76**, A7A13.